

Supporting information

Current-Voltage Characteristics and Transition Voltage Spectroscopy of Individual Redox Proteins

Juan M. Artés^{1,2}, Montserrat López-Martínez^{1,2}, Arnaud Giraudet[†], Ismael Díez-Pérez², Fausto Sanz^{1,2,3} and Pau Gorostiza^{1,3,4*}

1. Institute for Bioengineering of Catalonia (IBEC), Baldiri Reixac 15-21, Barcelona 08028 Spain
2. Physical Chemistry Department, University of Barcelona (UB), Martí i Franquès 1-11, Barcelona 08028 Spain
3. Networking Research Center on Bioengineering, Biomaterials and Nanomedicine (CIBER-BBN)
4. Institució Catalana de Recerca i Estudis Avançats (ICREA)

Present Addresses

[†]UNAM, Université de Nantes, Polytech Nantes, BP 50609, 44306 Nantes Cedex 3, France.

1. Experimental

Sample Preparation

Reported protocols were used to prepare atomically flat gold surfaces¹ and to attach azurin on gold² through native cysteines C3 and C26, which results in a defined orientation of the protein on the surface, while preserving its native-like conformation³ and electrochemical properties.^{4,5} Azurin and all reagents were purchased from Sigma.

Current Voltage and Transition Voltage Spectroscopy in spontaneously formed Single-Protein Junctions (wired configuration) and in tunneling configuration.

All experiments were performed with a PicoSPM microscope head and a PicoStat bipotentiostat (Molecular Imaging, USA) controlled by Dulcinea electronics (Nanotec Electronica, Spain) using WSxM 4.0 software.⁶ A homemade electrochemical cell was used

in four-electrode configuration, using a Pt:Ir (80:20) wire as counter electrode and a miniaturized ultralow leakage membrane Ag/AgCl (SSC) reference electrode filled with 3 M KCl. The potentials of the gold electrode sample (U_S) and ECSTM probe (U_P) are expressed against this reference. ECSTM cell and all of the glass material used for preparation of solutions were cleaned with piranha solution (7:3 H_2SO_4/H_2O_2 (30%) by volume). **Caution:** *Piranha solution should be handled with extreme caution.* Deionized water (18 M Ω cm⁻¹ Milli-Q, Millipore) was used to prepare all solutions and for rinsing samples and electrodes. Solution for experiments was 50 mM ammonium acetate buffer at pH 4.55. ECSTM probes were prepared by cutting a 0.025 mm diameter Pt:Ir (80:20) wire, briefly flame annealed and isolated with Apiezon wax. Data was acquired using a NI-DAQmx and BNC-2110 Labview equipment and analyzed with Origin. Current-time STM recordings⁷ were used in order to obtain spontaneous single wired protein junctions. In this case, after bringing the probe to tunneling distance to the substrate, the STM feedback was turned off and the current as function of time was recorded. When a molecule bridges probe and sample electrodes, a sudden “jump” or “blink” in the current is detected (I_{blink}). The magnitude of the blink can be used to calculate single protein conductance using $G = I_{blink}/U_{bias}$. This method has a relatively low success rate but has the advantage of allowing further experiments in single spontaneously wired junctions. As previously discussed, the interaction of azurin with the ECSTM tip involves residues in the region comprised between residues 35-48, and Lys41 is the best candidate for a covalent bond.⁸

For instance in the experiments reported here, an ECSTM probe potential ramp (U_P) was automatically triggered upon detection of azurin bridge formation, while the current signal was recorded.⁸ Experiments were performed at 25 ± 2 °C.

Single-molecule electrochemical recordings in tunneling regime were performed after a brief scanning of the sample (see Figure S1). The probe scanning was stopped at a current

S2

setpoint of 0.5nA, and the STM feedback was briefly turned off during the application of a 0.5V symmetric ramp to U_p . The difference between the initial setpoint current and its value at the end of the ramp (upon restoring the initial U_p , prior to resuming feedback) was taken as a measure of the vertical drift of the probe during the tunneling I-V recording (Figure 1b). Curves were automatically discarded if the deviation was higher than 10%, which greatly enhanced reproducibility (a 10% deviation of a 0.5 nA tunneling current corresponds to vertical drift of 0.03nm during the I-V curve). By comparison of the obtained population with clean Au control experiments, individual I-V curves were pooled and averaged. TVS representations were obtained by two alternative methods. I-V reference curves (with the ECSTM probe far from the surface) were subtracted from the individual I-V curves in tunneling regime in order to remove electrochemical background currents as previously described⁹. Curves were then smoothed using an adjacent averaging method with a 5000 points window (see example in Fig S4). The obtained smoothed data was used to produce the TVS representation ($\ln(I/V^2)$ vs $1/V$, see figure 2 in main text and figure S6c). In an alternative approach, the numerical version¹⁰ of the 2-step ET formalism¹¹ was used to fit individual I-V curves (see example in Fig S5). The resulting equation was then represented in the TVS context ($\ln(I/V^2)$ vs $1/V$, see figure 2 in main text and figures S6a and e). The minima found in the plots correspond to the TV in each case.

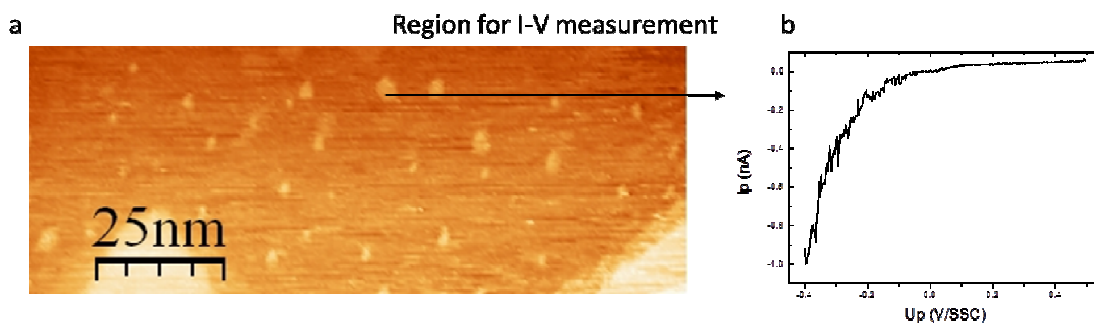


Figure S1. (a). ECSTM image of Azurin bound to Au<111> in 50 mM ammonium acetate pH 4.5 buffer. Current setpoint was 1 nA, $U_s=0.2$ V and $U_p=-0.4$ V. (b) Example of current Voltage curve recorded while disabling the feedback loop in the region shown in (a).

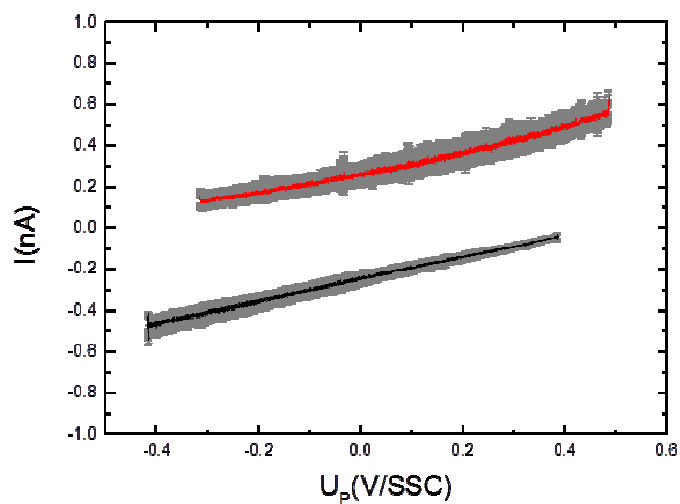


Figure S2. Averages of Current-Voltage curves performed in a control clean Au<111> surface in 50 mM ammonium acetate pH 4.5 buffer. Current setpoint was 0.5 nA, $U_s=0.2$ V, initial $U_p=-0.4$ V (black) and $U_s=-0.3$ V initial $U_p=0.5$ V (red). Gray bars indicate standard deviation. $N=20$ measurements.

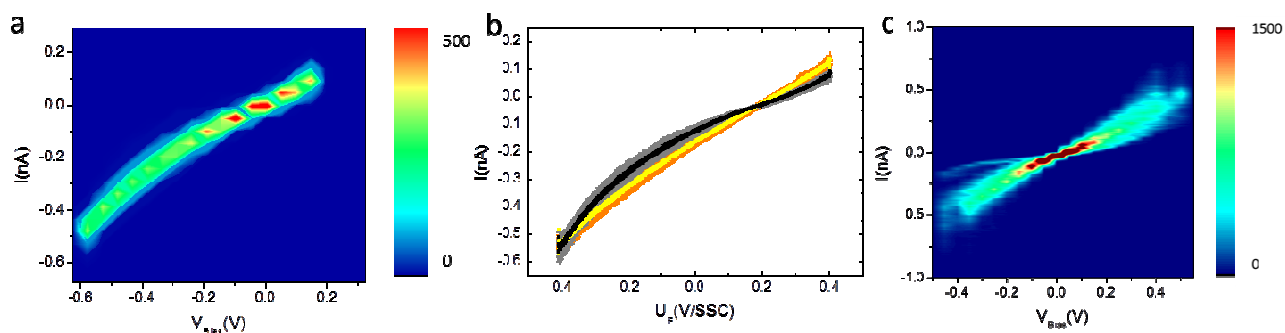


Figure S3. (a) 2-D histogram of I-V curves as a function of bias voltage obtained at $U_s=0.2$ V (oxidized azurin) and initial $U_p=-0.4$ V. Current setpoint is 0.5 nA. (b) Averages of I-V curves performed at
S4

$U_s=0.2\text{V}$, initial $U_p=-0.4\text{V}$ and current setpoint 0.5 nA , in 50 mM ammonium acetate pH 4.5 buffer. Rectifying curves (black) are not present in clean gold samples (Fig S2) and are attributed to tunneling through azurin. Azurin curves (black) and gold curves (yellow) were pooled and represented separately. Error bars indicate standard deviation. $N=10$ measurements. (c) 2-D histogram of I-V curves as a function of bias voltage obtained at $U_s=0\text{ V}$ (an intermediate potential close to azurin redox midpoint). Current setpoint is 0.5 nA .

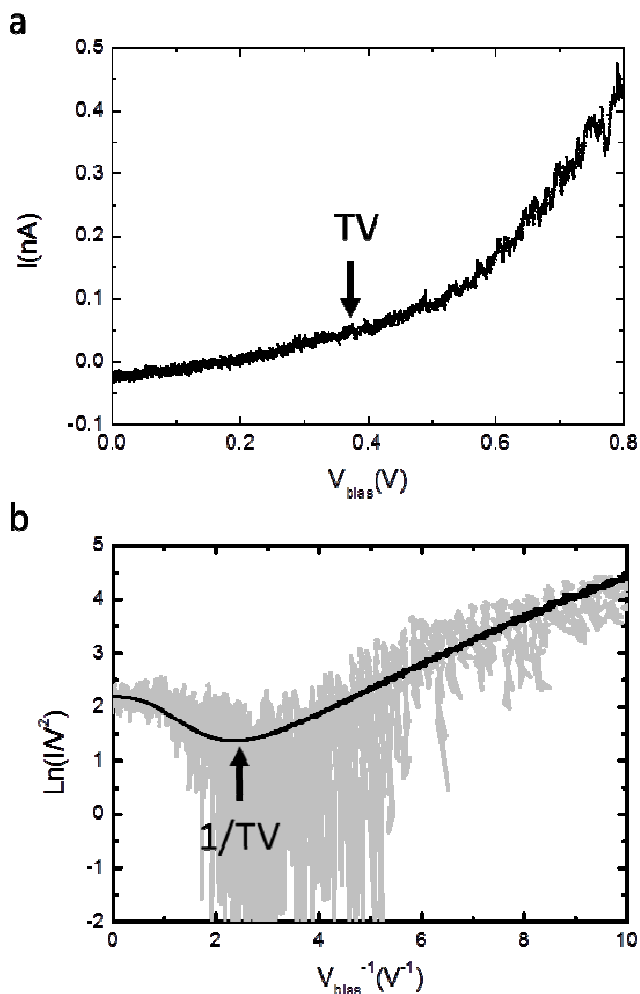


Figure S4. (a) Example of unprocessed I-V curve obtained at $U_s=-0.3\text{ V}$ and initial $U_p=0.5\text{ V}$, showing strong rectification associated to azurin.

(b) TVS representation ($\ln(I/V^2)$ vs $1/V$) of the raw data (in gray) and smoothed data (in black), providing $TV \approx 0.37\text{ V}$.

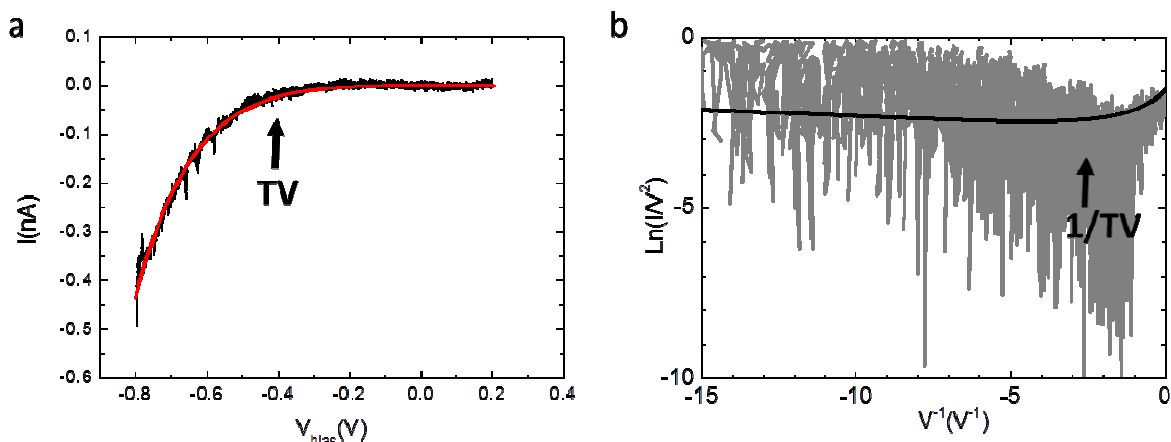


Figure S5. (a) Example fit of an individual I-V curve on azurin ($U_S=0.2V$, initial $U_P=-0.4V$, setpoint $0.5nA$, black plot) to the numerical expression¹⁰ of the 2-step ET formalism¹¹ (red plot). (b) TVS representation of the fitting (black line) and the raw data (gray) in (a). $TV = 0.37 V$.

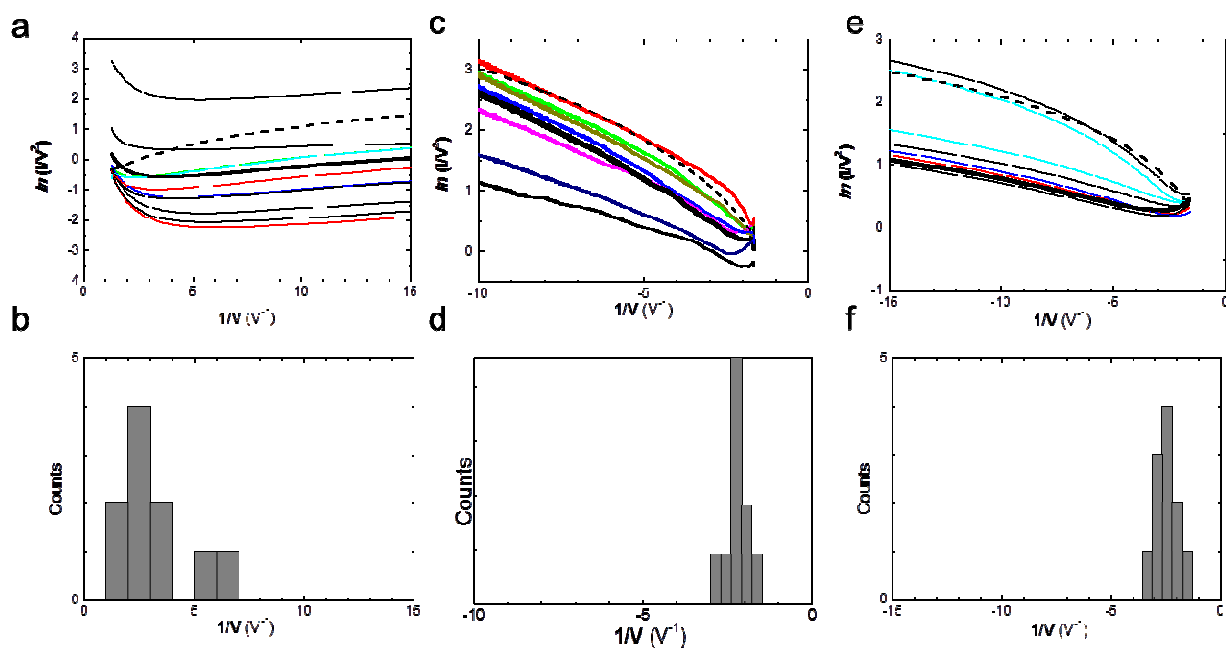


Figure S6. (a) TVS representation of individual fittings of the numerical expression¹⁰ for a 2-step ET¹¹ performed on I-V curves attributed to azurin at $U_S=-0.3V$, initial $U_P=0.5V$. Thick line indicates the TVS representation of the average of all the I-V curves. Dashed line shows the Au control I-V average for comparison. (b) Histogram of the TV minima obtained from (a). (c) TVS representation of smoothed I-V curves obtained at $U_S=0.2V$, initial $U_P=-0.4V$. Thick line indicates the TVS representation of the average of all the I-V curves. Dashed line shows the Au control I-V average for comparison. (d) TV histogram obtained from (c). (e) TVS representation of individual fittings of the numerical expression¹⁰ for a 2-step ET¹¹ performed on I-V curves attributed to azurin at $U_S=0.2V$, initial $U_P=-0.4V$. Thick line indicates the TVS representation of the average of all the I-V curves. Dashed line

shows the Au control I-V average for comparison. (f) TV histogram obtained from (e). The TVS values obtained are shown in Table S1.

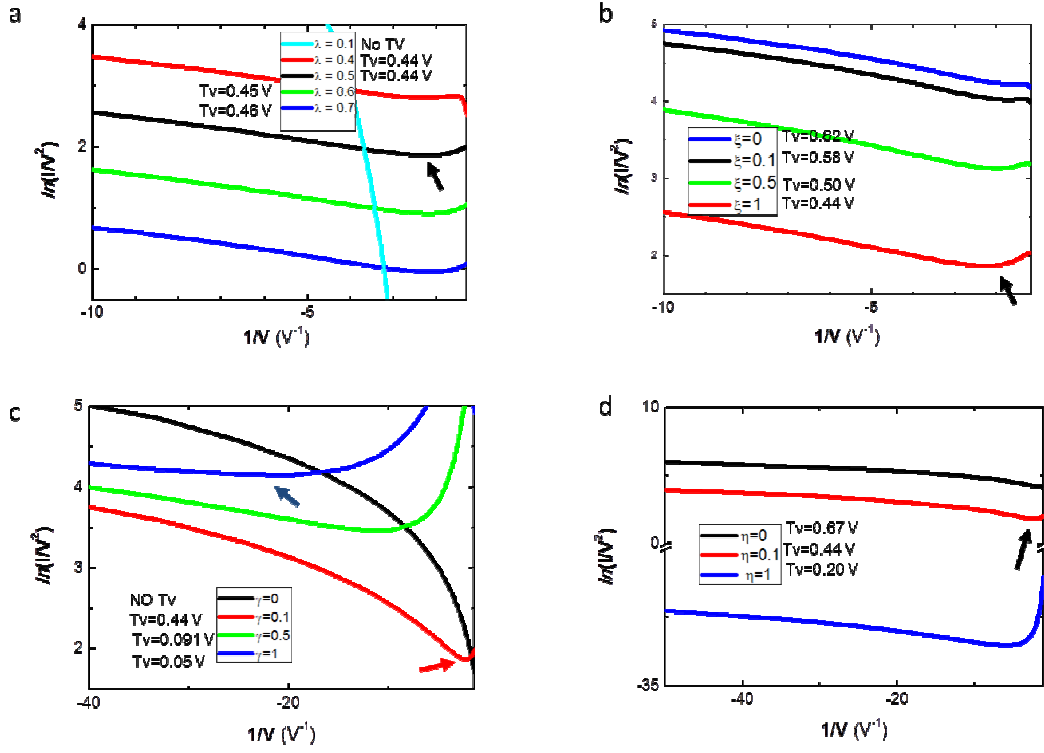


Figure S7. (a) TVS numerical simulation of the two-step ET formalism¹¹ at fixed $\kappa=1$, $\xi=1$, $\gamma=0.1$, $\eta=0.2$ V and different reorganization energies indicated in the inset legend, together with the TV values obtained in each case. (b) TVS simulations at fixed $\kappa=1$, $\lambda=0.5$, $\gamma=0.1$, $\eta=0.2$ V and different substrate coupling parameters indicated in the inset, together with the obtained TV. (c) TVS simulations at fixed $\kappa=1$, $\lambda=0.5$, $\xi=1$, $\eta=0.2$ V and different probe coupling parameters indicated in the inset, together with the obtained TV. (d) TVS simulations at fixed $\kappa=1$, $\lambda=0.5$, $\xi=1$, $\gamma=0.1$ and different overpotentials indicated in the inset, together with the obtained TV. In all cases, the minimum in the curve equivalent to the experimental conditions is indicated with a black arrow. In (c) the blue arrow indicates the minimum equivalent to the wired configuration and the red arrow corresponds to the tunneling configuration.

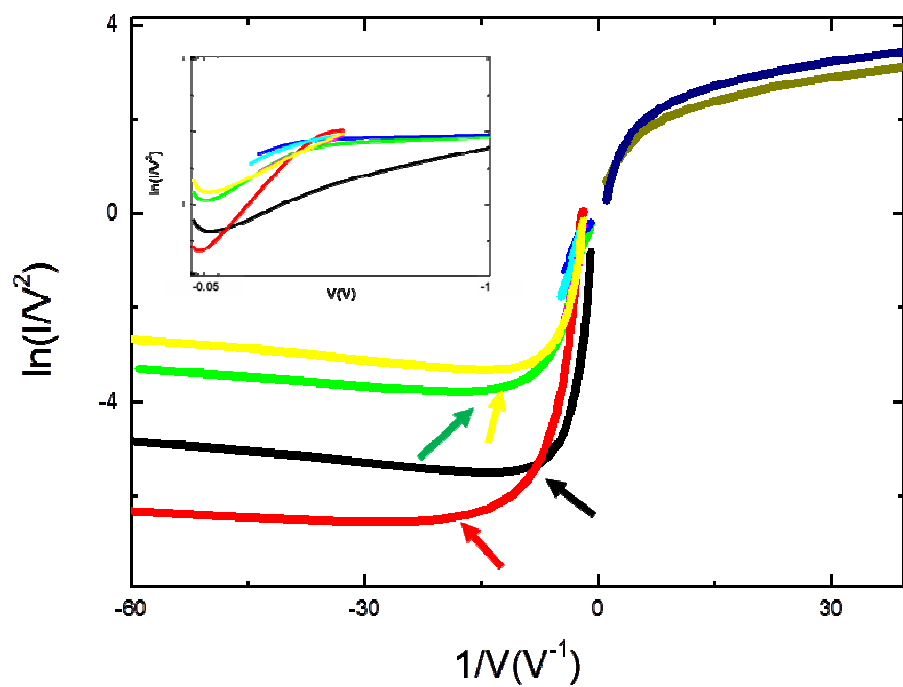


Figure S8. TVS plots of two-step $ET^{10,11}$ fits of individual I-V curves of azurin in wired junctions.⁸ Examples of minima in some of the curves are indicated with arrows. Inset shows the same data in a reciprocal axis (V) for clarity.

REFERENCES

- (1) Nagy, G.; Wandlowski, T. *Langmuir* **2003**, *19*, 10271.
- (2) Friis, E. P.; Andersen, J. E. T.; Madsen, L. L.; Moller, P.; Ulstrup, J. *Journal of Electroanalytical Chemistry* **1997**, *431*, 35.
- (3) Pompa, P. P.; Bramanti, A.; Maruccio, G.; Cingolani, R.; De Rienzo, F.; Corni, S.; Di Felice, R.; Rinaldi, R. *Journal of Chemical Physics* **2005**, *122*.
- (4) Alessandrini, A.; Corni, S.; Facci, P. *Physical Chemistry Chemical Physics* **2006**, *8*, 4383.
- (5) Chi, Q. J.; Zhang, J. D.; Friis, E. P.; Andersen, J. E. T.; Ulstrup, J. *Electrochemistry Communications* **1999**, *1*, 91.
- (6) Horcas, I.; Fernandez, R.; Gomez-Rodriguez, J. M.; Colchero, J.; Gomez-Herrero, J.; Baro, A. M. *Review of Scientific Instruments* **2007**, *78*.
- (7) Haiss, W.; Nichols, R. J.; van Zalinge, H.; Higgins, S. J.; Bethell, D.; Schiffrin, D. J. *Physical Chemistry Chemical Physics* **2004**, *6*, 4330.
- (8) Artes, J. M.; Diez-Perez, I.; Gorostiza, P. *Nano letters* **2012**, *12*, 2679.
- (9) Diez-Perez, I.; Guell, A. G.; Sanz, F.; Gorostiza, P. *Analytical Chemistry* **2006**, *78*, 7325.
- (10) Pobelov, I. V.; Li, Z. H.; Wandlowski, T. *Journal of the American Chemical Society* **2008**, *130*, 16045.
- (11) Kuznetsov, A. M.; Ulstrup, J. *Electrochimica Acta* **2000**, *45*, 2339.